

Denoising Process Based on Arbitrarily Shaped Windows

Huda Al-Ghaib

*Assistant Professor/Computer Science/Technology and Computing
Utah Valley University
Orem, 84058, USA*

Huda.Ghaib@uvu.edu

Reza Adhami

*Professor/Electrical and Computer Engineering
University of Alabama in Huntsville
Huntsville, 35899, USA*

adhamir@uah.edu

Abstract

Many factors, such as moving objects, introduce noise in digital images. The presence of noise affects image quality. The image denoising process works on reconstructing a noiseless image and improving its quality. When an image has an additive white Gaussian noise (AWGN) then denoising becomes a challenging process. In our research, we present an improved algorithm for image denoising in the wavelet domain. Homogenous regions for an input image are estimated using a region merging algorithm. The local variance and wavelet shrinkage algorithm are applied to denoise each image patch. Experimental results based on peak signal to noise ratio (PSNR) measurements showed that our algorithm provided better results compared with a denoising algorithm based on a minimum mean square error (MMSE) estimator.

Keywords: Region Merging, Wavelet Transform, Image Denoising, Noise Estimation, Wavelet Shrinkage Process.

1. INTRODUCTION

Digital images have numerous applications in areas such as medical imaging, biometrics, robotics, and image navigation [1]. Some examples of medical imaging are computed tomography scan (CT), magnetic resonance imaging (MRI), ultrasound, X-ray, myocardial perfusion, and mammography. Medical imaging devices have helped physicians diagnose different diseases at early stages. In some cases, medical images may be noisy due to factors such as patient movement during the imaging process [2]-[4]. Noise presented in a digital image affects its quality. Noise occurs during image acquisition and/ or transmission. In most cases, noise originates from an unknown source and location. In this case, the noise is assumed to be an additive white Gaussian noise (AWGN) of unknown mean and variance. Accurate estimation of noise parameters is a preliminary step in a successful denoising process.

The main goal of the presented research is to provide a method to denoise digital images using accurate estimations of noise variance. The denoising process is applied on local image patches. First, an input image is subdivided into a number of patches. For each patch, the local variance is estimated and used to denoise the image using a wavelet shrinkage denoising algorithm. Noise estimation and elimination are executed in the wavelet domain.

2. MATERIALS and METHODS

2.1 The Proposed Algorithm

AWGN presented in digital images is of an additive nature. Differentiation of image information and noise is a challenging procedure. AWGN is characterized by its mean and variance. In most cases, AWGN is assumed to possess a mean of zero. In our research, wavelet transform is

applied to decompose an input image of size $M \times N$ into high and low frequency components. The magnitude of the vertical and horizontal details is computed to produce an image, MAG , of size $M \times N$. MAG is subdivided into a number of sub images. For each sub image, region merging is computed to estimate the local variance using only the homogenous regions [5]. The region merging algorithm is explained in detail in Section 2.2. A wavelet shrinkage process, explained in Section 2.3, is applied to denoise the sub image using the estimated variance [6].

2.2 Local Noise Estimation Using The Region-Merging Algorithm

An image I is subdivided into $M \times M$ windows. Next, R window is subdivided into Q sub windows as shown in Figure 1. Where r_0, \dots, r_{Q-1} are the sub windows each of size $m \times m$. r_0 is the sub window at the center in R . For each sub window in R , the following two conditions must be satisfied:

1. $r_i \cap r_j = \emptyset$, for $i \neq j$.
2. $\cup_i r_i = R$.

where $M = 9$, $m = 3$, and $Q = 9$.

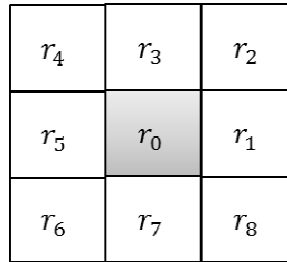


FIGURE 1: Region R of size 9×9 .

The variance for the pixels within r_0 is σ_0^2 and is considered as the seed sub window in R . Other adjacent sub windows are merged with r_0 if they pass the homogeneity test. The homogeneity test is computed as:

$$h_q = \frac{|\sigma_q^2 - \sigma_0^2|}{\sigma_0^2}, q = 0, 1, \dots, Q - 1 \tag{1}$$

where σ_q^2 is the variance of r_q . Each sub window is assumed to be of zero mean and the variance is computed as:

$$\sigma_q^2 = \frac{1}{|c_q|} \sum_{y_m \in c_q} y_m^2 \tag{2}$$

where c_q is the coefficient within r_q . The following condition is applied to test h_q :

$$m_q = \begin{cases} 1, & \text{if } h_q < t \\ 0, & \text{otherwise} \end{cases} \tag{3}$$

where $t = 0.2$. If $m_q = 1$ for a given r_q , then r_q is merged with r_0 , otherwise it is discarded. The homogeneity test is performed on every sub window in R . As a result, final R is of an arbitrary shape. When $Q = 9$, there are $2^{Q-1} = 256$ different configurations for R . Figure 2 shows some possible configurations for R .

The local noise variance for the merged sub windows is computed as:

$$\hat{\sigma}_k^2 = \left(\frac{\sum_{q=0}^{Q-1} \sigma_{k,q}^2 \cdot m_{k,q}}{\sum_{q=0}^{Q-1} m_{k,q}} - \sigma_n^2 \right) \quad (4)$$

where σ_n^2 is the global noise variance estimated using a variation-adaptive evolutionary approach [5]. Equation (4) is applied on each image patch.

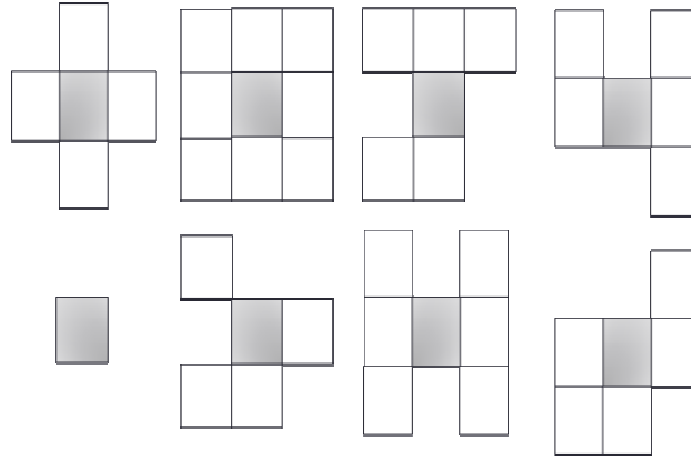


FIGURE 2: Local windows with arbitrary size and shape; r_o is the gray-scale region.

2.3 The Denoising Algorithm

A wavelet shrinkage denoising operator can be defined as [24]:

$$C(x) = \text{sign}(x) \begin{cases} |x| - T_n, & |x| \geq T_n \\ 0, & \text{otherwise} \end{cases} \quad (5)$$

Since x is the magnitude of the detail coefficients and is always ≥ 0 , equation (5) can be rewritten as:

$$C(M) = \begin{cases} M - T_n, & M \geq T_n \\ 0, & \text{otherwise} \end{cases} \quad (6)$$

The function $C(M)$ must satisfy the following two conditions:

1. Being a piece wise linear function.
2. Being a monotonically non-decreasing function.

T_n is the threshold value. An accurate estimation for T_n is needed to have an efficient denoising process. Reference [8] suggested the following mathematical model to compute T_n as:

$$T_n = \sqrt{2 \ln(N)} \sigma / \sqrt{N} \quad (7)$$

N is the signal length and σ is the standard deviation of the wavelet coefficients. However, equation (7) cannot be applied to our algorithm for the following reasons:

1. It uses a non-orthogonal UWT.
2. The shrinkage operation is applied to the magnitudes of the gradient coefficients instead of the wavelet coefficients.

For a white Gaussian noise, the probability distribution function of the magnitude of gradients is characterized by the Rayleigh distribution as [8]:

$$Pr_{||\Delta f||}(m) = \begin{cases} \frac{m}{\eta^2} e^{-\frac{(m)^2}{\eta^2}} / 2, & m \geq 0 \\ 0, & m < 0 \end{cases} \quad (8)$$

As a result, there is a direct relationship between σ and η , where σ and η are the standard deviations for the Gaussian and Rayleigh distributions respectively. Thus, equation (7) can be rewritten as:

$$T_n = \eta \sqrt{-2 \ln(1 - p)} \quad (9)$$

p is the probability of noise removal for a particular threshold T_n and is computed as:

$$p = \frac{\int_0^{T_n} Pr_{||\Delta f||}(m) dm}{\int_0^{\infty} Pr_{||\Delta f||}(m) dm} \quad (10)$$

Based on Equation (10), $T_n = 3.7169\eta$ for $p = 0.999$, and $T_n = 4.5\eta$ for $p = 0.99996$. In [6] and [8] η is computed using the histogram of $||\Delta f||$ and an iterative curve fitting function. In our paper we applied a novel approach based on ACO to achieve an accurate estimation of η [7].

2.4 Error Rate for σ Estimation

A set of images was used as experimental input to test the noise variance estimation algorithms. These images are: Lena, cameraman, barbara, kodim05, kodim06, kodim07, kodim08, kodim21, and kodim24, Figure 3 shows the input images. AWGN with different standard deviation values were added to the input images, i.e., $\sigma = 80.6, 71.4, 57, 51$ and 25.5 respectively. This produced images of high noise density. Noise variance is estimated using a variation-adaptive evolutionary approach [7]. Table I displays the averaged normalized values for the noise variance, i.e., added and estimated. Table II displays the averaged error rate for the estimated noise variance for the input images. Even though the added noise possesses high standard deviations, it is obvious from Tables I and II that the estimation process is of low error rate.



FIGURE 3: Input Images.

TABLE 1: Noise Variance Estimation.

σ^2 (Added)	0.1	0.078	0.05	0.04	0.01
σ^2 (Estim.) ACO	0.082	0.068	0.059	0.048	0.028

TABLE 2: Mean and variance of error rate: Comparison for different noise estimation algorithms.

σ^2	Mean of error rate	Variance of error rate
0.1	0.0197	1.2419e-005
0.0784	0.0108	1.2535e-005
0.05	0.0034	1.1162e-005
0.04	0.0055	3.6346e-005
0.01	0.0035	5.3444e-006

3. EXPERIMENTAL RESULTLS

The noisy images, along with the estimated noise variance, are used as inputs for the denoising algorithm. Wavelet transform is applied to decompose the input image. The algorithm is performed on the magnitude of the horizontal and vertical details. The algorithm explained in Section 2.3 is implemented to estimate the local variance for each image patch. The local denoising process is applied using the denoising algorithm explained earlier in Section 2.3. Denoising is performed twice using a minimum mean square error (MMSE) estimator and wavelet shrinkage algorithm respectively. The peak signal to noise ratio (PSNR) is computed for the noisy and denoised images, and the results are presented in Table III. Notations (1) and (2) in Table III illustrate wavelet-based denoising based on a MMSE estimator and our algorithm respectively. From Table III it is obvious that our improved algorithm provided better results compared with the original algorithm based on using a MMSE estimator [5]. These results showed that MMSE provided slightly better results in only 10 cases compared with our algorithm. Our algorithm accuracy is 78.78%.

4. CONCLUSION

This research provided an improved denoising algorithm based on wavelet shrinkage operation. A region merging algorithm is developed in the wavelet domain to locate the homogenous regions. The local homogenous regions are applied to estimate the local variance to denoise the region using the region merging algorithm. Experimental results based on PSNR illustrated in Table III showed that our improved algorithm provided better results compared with minimum mean square error (MMSE) in 78.78% of the cases.

5. REFERENCES

- [1] H. Al-Ghaib and R. Adhami, *An E-learning interactive course for teaching digital image processing at the undergraduate level in engineering*, Interactive Collaborative Learning (ICL), 2012 15th International Conference on, vol.1, no.5, pp.26-28, September 2012.
- [2] R. Eisenberg and A. Margulis. *A Patient's Guide To Medical Imaging*. New York, Oxford University Press, 2011.
- [3] U. Bhowmik, M. Iqbal, and R. Adhami, Mitigating motion artifact in FDK based 3D Cone-beam Brain Imaging System using markers, *Central European Journal of Engineering*, vol.2, no.3, pp.369-382.
- [4] U. Bhowmik and R. Adhami, A Novel Technique for Mitigating Motion Artifacts in 3D Brain Imaging System, *Scientific Iranica*, vol.20, no.3, pp.746-759, March 2013.

- [5] I. Kyu and Y. Kim, Wavelet-based denoising with nearly arbitrarily shaped windows, *Signal Processing Letters, IEEE*, vol.11, no.12, pp.937-940, December 2004.
- [6] A. Mencattini, M. Salmeri, R. Lojacono, M. Frigerio, and F. Caselli, Mammographic Images Enhancement and Denoising for Breast Cancer Detection Using Dyadic Wavelet Processing, *Instrumentation and Measurement, IEEE Transactions on*, vol.57, no.7, pp.1422-1430, July 2008.
- [7] J. Tian and L. Chen, Image Noise Estimation Using A Variation-Adaptive Evolutionary Approach, *Signal Processing Letters, IEEE* , vol.19, no.7, pp.395-398, July 2012.
- [8] J. Fan and A. Laine, Contrast enhancement by multiscale and nonlinear operators, *Wavelets in Medicine and Biology.*, pp. 163-192. Boca Raton, FL: CRC, March 1996.

TABLE 3: PSNR for Noisy and Denoised Images.

σ^2 (Added)	0.1	0.078	0.05	0.04	0.01
Estimated σ^2 , Lena	0.08	0.07	0.046	0.039	0.014
PSNR -noisy Lena	14.25	15.04	16.58	17.41	23.07
PSNR- denoised Lena(1)	23.02	23.09	25.94	25.31	31.5
PSNR- denoised Lena(2)	20.93	20.15	20.22	22.99	27.83
Estimated σ^2 , cameraman	0.082	0.067	0.05	0.056	0.022
PSNR- noisy cameraman	14.34	15.2	16.61	17.42	23.05
PSNR- denoised cameraman (1)	22.08	22.47	24.69	23.94	29.25
PSNR- denoised cameraman (2)	19.17	20.06	22.04	22.04	26.36
Estimated σ^2 , barbara	0.08	0.07	0.05	0.04	0.02
PSNR- noisy barbara	14	14.78	16.4	17.27	23.03
PSNR- denoised barbara (1)	23.17	23.6	25.16	25.93	32.58
PSNR- denoised barbara (2)	20.91	22.64	21.25	23.12	28.32
Estimated σ^2 , kodim05	0.08	0.067	0.047	0.05	0.037
PSNR-noisy kodim05	13.53	14.47	16.28	17.17	23.08
PSNR-denoised kodim05 (1)	25.02	24.61	26.62	27.1	27.86
PSNR-denoised kodim05 (2)	23.27	22.95	24.76	24.32	27.51
Estimated σ^2 , kodim06	0.09	0.07	0.054	0.04	0.02
PSNR- noisy kodim06	14.67	15.5	17.7	17.95	23.56
PSNR-denoised kodim06 (1)	19.03	20.45	21.95	21.43	23.56
PSNR-denoised kodim06 (2)	16.89	18.64	19.03	19.95	21.66
Estimated σ^2 , kodim07	0.08	0.068	0.048	0.041	0.016
PSNR- noisy kodim07	13.83	14.6	16.25	17.15	23.03
PSNR- denoised kodim07 (1)	23.55	26.89	26.4	27.1	28.04
PSNR- denoised kodim07 (2)	21.99	21.84	22	24.48	27.51
Estimated σ^2 , kodim08	0.09	0.07	0.06	0.06	0.06
PSNR- noisy kodim08	23.42	15.28	16.92	17.8	23.45
PSNR- denoised kodim08 (1)	23.21	20.21	20.4	21.85	22.73
PSNR- denoised kodim08 (2)	17.74	18.84	19.1	18.55	21.37
Estimated σ^2 , kodim21	0.08	0.07	0.05	0.04	0.03
PSNR- noisy kodim21	13.96	14.77	16.39	17.2	23.1
PSNR- denoised kodim21 (1)	23.42	23.54	23.76	25.17	27.5
PSNR- denoised kodim21 (2)	20.5	20.96	22.7	22.96	23.57
Estimated σ^2 , kodim24	0.08	0.07	0.05	0.04	0.025
PSNR-noisy kodim24	13.92	14.79	16.53	17.43	23.35
PSNR- denoised kodim24 (1)	21.55	21.84	22.17	22.41	23.43
PSNR- denoised kodim24 (2)	19.01	20.4	19.77	20.63	22.12